B, $B_s \to K$ form factors: An update of light-cone sum rule results

Goran Duplančić* and Blaženka Melić+

Theoretical Physics Division, Rudjer Boskovic Institute, Bijenička 54, HR-10002 Zagreb, Croatia

(Received 29 May 2008; revised manuscript received 14 August 2008; published 16 September 2008)

We present an improved QCD light-cone sum rule (LCSR) calculation of the $B \to K$ and $B_s \to K$ form factors by including SU(3)-symmetry breaking corrections. We use recently updated K meson distribution amplitudes which incorporate the complete SU(3)-breaking structure. By applying the method of direct integration in the complex plane, which is presented in detail, the analytical extraction of the imaginary parts of LCSR hard-scattering amplitudes becomes unnecessary and therefore the complexity of the calculation is greatly reduced. The values obtained for the relevant $B_{(s)} \to K$ form factors are as follows: $f^+_{BK}(0) = 0.36^{+0.05}_{-0.04}$, $f^+_{B_sK}(0) = 0.30^{+0.04}_{-0.03}$, and $f^T_{BK}(0) = 0.38 \pm 0.05$, $f^T_{B_sK}(0) = 0.30 \pm 0.05$. By comparing with the $B \to \pi$ form factors extracted recently by the same method, we find the following SU(3) violation among the $B \to$ light form factors: $f^+_{BK}(0)/f^+_{B\pi}(0) = 1.38^{+0.11}_{-0.10}$, $f^+_{B_sK}(0)/f^+_{B\pi}(0) = 1.15^{+0.17}_{-0.09}$, $f^T_{BK}(0)/f^T_{B\pi}(0) = 1.49^{+0.18}_{-0.06}$, and $f^T_{B_sK}(0)/f^T_{B\pi}(0) = 1.17^{+0.15}_{-0.11}$.

DOI: 10.1103/PhysRevD.78.054015 PACS numbers: 13.25.Hw, 12.38.Lg

I. INTRODUCTION

The $B \to$ light meson form factors are important ingredients in the analysis of semileptonic B decays, as well as of nonleptonic two-body B decays, where they serve for extraction of the Cabibbo-Kobayashi-Maskawa matrix elements. They have been studied by light-cone sum rule (LCSR) [1] methods in several papers [2–13], and most recently in [14]. In this paper we want to concentrate on the flavor SU(3)-symmetry breaking corrections in $B \to K$ and $B_s \to K$ form factors, closely following the method presented in [14]. In [14], the $B \to \pi$ form factors were analyzed, and in contrast to the previous calculations with the pole mass for m_b, the $\overline{MS}$ mass $\bar{m}_b(\mu)$ was used. This choice more naturally follows the idea of the perturbative calculation of the hard-scattering amplitudes. Since the sum rule calculation of f_B and f_{B_s} decay constants is also available in the $\overline{MS}$ scheme [15], we are able to consistently perform estimation of the $f_{B_{(s)}K}$ form factors in this scheme.

The notion of SU(3) breaking is particularly interesting in a view of discrepancies of measured values for $B_{(s)} \to \pi K$ decay widths and CP asymmetries compared to standard model predictions. The $B_{(s)} \to K$ transition form factors enter different models for calculating these decays, and according to the recent analysis [16], one solution of these discrepancies is given by assuming the large SU(3)-breaking effects, either in strong phases or in amplitudes. Our intention is to calculate these effects in different $B_{(s)} \to K$ form factors by using all known SU(3)-breaking corrections in the parameters and in distribution amplitudes (DAs) entering the LCSR calculation.

Up to now, in [9,17,18], the main SU(3)-breaking effects were included by considering SU(3)-breaking in the parameters of the leading twist DAs, such as f_K/f_π and μ_K/μ_π, and by inserting $p^2 = m_K^2 \neq 0$ at LO. In the meantime, the complete SU(3)-symmetry breaking corrections in the K meson DAs are known [19]. In [19], the authors complete the analysis of SU(3)-breaking corrections done in [20–24], for all twist-3 and twist-4 two- and three-particle DAs, by including also G-parity-breaking corrections in $m_s - m_q$. Therefore our analysis will include complete SU(3)-breaking effects in both kaon DAs, as well as in the hard-scattering amplitudes at LO. At next-to-leading order (NLO) in the hard-scattering amplitudes, the inclusion of m_s and m_K^2 effects complicates the calculation. Because of the complexity of mixing between twist-2 and twist-3 DAs, we were not able to perform consistent calculations with m_s included in the quark propagators. Therefore, in those amplitudes we also set $p^2 = m_K^2 = 0$, and consistently use twist-2 and twist-3 two-particle kaon DAs without mass corrections. However, we analyze the kaon mass effects ($p^2 = m_K^2$) at NLO and include them in the error estimates. More detailed discussion about this point will be given in Sec. II.

Since the LO hard-scattering amplitudes are already complicated when the twist-4 and three-particle DAs are included, we will use the new, numerical method to calculate the sum rules. The idea is to use the analyticity of the integrals, and to continue them to the complex plane. The integrals are then performed over the contour in a complex plane, and the imaginary part is obtained numerically. The details of the method will be given below.

II. LCSR FOR $B_{(s)} \to K$ FORM FACTORS

To obtain the form factors f^+_{BK}, f^0_{BK}, and f^T_{BK} from LCSR we consider the vacuum-to-kaon correlation func-

*gorand@thphys.irb.hr
+melic@thphys.irb.hr

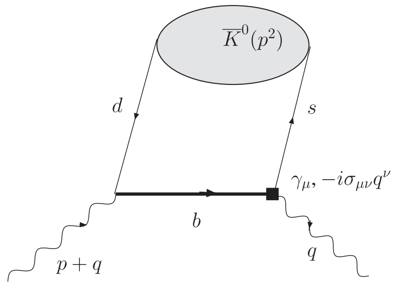

FIG. 1. Diagrams corresponding to the leading-order terms in the hard-scattering amplitudes involving the two-particle (left) and three-particle (right) kaon DA's shown by ovals. Solid, curly, and wavy lines represent quarks, gluons, and external currents, respectively. In the case of the $B_s \to K$ transition, s and d quarks are interchanged, and $\bar{K}^0$ is replaced by K^0.

tion of a weak current and a current with the B meson quantum numbers:

$$F_\mu(p, q) = i \int d^4x e^{iq\cdot x} \langle K(p)|T\{\bar{s}(x)\Gamma_\mu b(x), m_b \bar{b}(0) i\gamma_5 d(0)\}|0\rangle = \begin{cases} F(q^2, (p+q)^2)p_\mu + \tilde{F}(q^2, (p+q)^2)q_\mu, & \Gamma_\mu = \gamma_\mu \\ F^T(q^2, (p+q)^2)[p_\mu q^2 - q_\mu(qp)], & \Gamma_\mu = -i\sigma_{\mu\nu}q^\nu \end{cases} \tag{1}$$

for the two different $b \to s$ transition currents. For definiteness, we consider the $\bar{B}_d \to \bar{K}^0(s\bar{d})$ flavor configuration, and use the isospin symmetry limit, ignoring replacement of a u quark by a d quark in the penguin current. For the case of $f^{+,0,T}_{B_s K}$ form factors we consider the $B_s \to K^0(\bar{s}d)$ decay. This enables us to use the same correlation function, with s and d quarks interchanged, but in the kaon DAs one has to take care about the fact that DAs from [19] are defined for the configuration in which the momentum fraction carried by the s-quark is u (i.e., α_1 in the three-particle DAs), and $\bar{u} = 1 - u$ (α_2 in the three-particle DAs) is the antiquark momentum fraction. Since we want to explore the SU(3)-breaking corrections we will keep the kaon mass ($p^2 = m_K^2$) and the m_s quark mass in the DAs. The light quark masses will be systematically neglected, except in the ratio $\mu_K = m_K^2/(m_s + m_d)$.

For the large virtualities of the currents above, the correlation function is dominated by the distances $x^2 = 0$ near the light cone, and factorizes to the convolution of the nonperturbative, universal part (the light-cone DA) and the perturbative, short-distance part, the hard-scattering amplitude, as a sum of contributions of increasing twist. In contrast to the pion DA, where due to the G-parity odd Gegenbauer moments vanish, the lowest twist-2 DA of a kaon has an expansion

$$\phi_K(u, \mu) = 6u(1-u)(1 + a_1^K(\mu)C_1^{3/2}(2u-1) + a_2^K(\mu)C_2^{3/2}(2u-1) + \ldots), \tag{2}$$

where we neglect higher moments $a^K_{>2}$. We calculate here contributions up to the twist-4 in the leading order ($O(\alpha_s^0)$) and up to the twist-3 in NLO, neglecting the three-particle contributions at this level. Schematically, the contributions are shown in Fig. 1 and 2.

By using the hadronic dispersion relation in the virtuality $(p+q)^2$ of the current in the B channel, we can relate the correlation function (1) to the $B \to K$ matrix elements,

$$\langle K(p)|\bar{s}\gamma_\mu b|\bar{B}_d(p+q)\rangle = 2f^+_{BK}(q^2)p_\mu + (f^+_{BK}(q^2) + f^-_{BK}(q^2))q_\mu, \tag{3}$$

$$\langle K(p)|\bar{s}\sigma_{\mu\nu}q^\nu b|\bar{B}_d(p+q)\rangle = [q^2(2p_\mu + q_\mu) - (m_B^2 - m_K^2)q_\mu]\frac{if^T_{BK}(q^2)}{m_B + m_K}. \tag{4}$$

Inserting hadronic states with the B-meson quantum numbers between the currents in (1), one isolates the B-meson ground-state contributions for all three invariant amplitudes $F(q^2, (p+q)^2)$, $\tilde{F}(q^2, (p+q)^2)$, and $F^T(q^2, (p+q)^2)$ and using (3) and (4) obtains

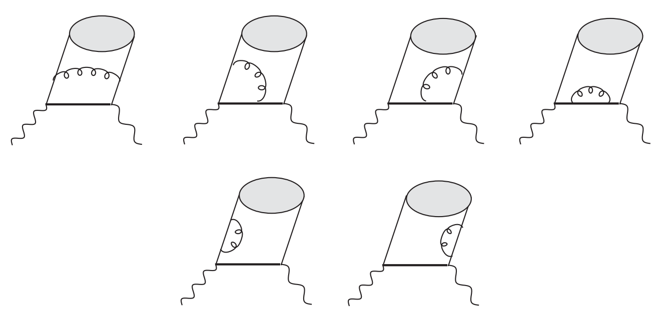

FIG. 2. Diagrams contributing to the hard-scattering amplitudes at $O(\alpha_s)$.

$$f^+_{BK}(q^2) = \frac{e^{m_B^2/M^2}}{2m_B^2 f_B}\bigg[F_0(q^2, M^2, s_0^B) + \frac{\alpha_s C_F}{4\pi} F_1(q^2, M^2, s_0^B)\bigg], \quad (5)$$

$$f^+_{BK}(q^2) + f^-_{BK}(q^2) = \frac{e^{m_B^2/M^2}}{m_B^2 f_B}\bigg[\tilde{F}_0(q^2, M^2, s_0^B) + \frac{\alpha_s C_F}{4\pi} \tilde{F}_1(q^2, M^2, s_0^B)\bigg], \quad (6)$$

$$f^T_{BK}(q^2) = \frac{(m_B + m_K)e^{m_B^2/M^2}}{2m_B^2 f_B}\bigg[F^T_0(q^2, M^2, s_0^B) + \frac{\alpha_s C_F}{4\pi} F^T_1(q^2, M^2, s_0^B)\bigg]. \quad (7)$$

The scalar $B \to K$ form factor is then a combination of the vector form factor (5) and the f^-_{BK} form factor from (6),

$$f^0_{BK}(q^2) = f^+_{BK}(q^2) + \frac{q^2}{m_B^2 - m_K^2} f^-_{BK}(q^2). \quad (8)$$

In the above, $F_{0(1)}$ and $\tilde{F}_{0(1)}$ represent the LO (NLO) contributions and $f_B = \langle \bar{B}_d | m_b \bar{b} i\gamma_5 d|0\rangle/m_B^2$ is the B-meson decay constant. As usual, the quark-hadron duality is used to approximate the heavier state contribution by introducing the effective threshold parameter s_0^B, and the ground-state contribution of B meson is enhanced by the Borel-transformation in the variable $(p+q)^2 \to M^2$. Completely analogous relations are valid for $B_s \to K$ form factors, with the replacement $s \leftrightarrow d$ in (3) and (4) and by replacing m_B by m_{B_s}, f_B by f_{B_s}, as well as M^2 by M_s^2 and s_0^B by $s_0^{B_s}$ in (5)–(7). In addition, in the derivation of the above expressions for B_s, one has to take into account that $\langle B_s|\bar{b} i\gamma_5 s|0\rangle/m_{B_s}^2 = f_{B_s}/(m_b + m_s)$.

The calculation will be performed in the $\overline{MS}$ scheme. The B and B_s decay constants $f_{B_{(s)}}$ will be calculated in the $\overline{MS}$ scheme using the sum rule expressions from [15] with $O(\alpha_s, m_s^2)$ accuracy.

Each form factor can be written in a form of the dispersion relation:

$$F(q^2, M^2_{(s)}, s_0^{B_s}) = \frac{1}{\pi}\int_{m_b^2}^{s_0^{B_{(s)}}} ds e^{-s/M^2_{(s)}} \mathrm{Im}_s F(q^2, s), \quad (9)$$

where now $s = (p+q)^2$. The leading-order parts of the LCSR for f^+_{BK}, $f^+_{BK} + f^-_{BK}$, and f^T_{BK} form factors have the following forms:

$$\begin{aligned}F_0(q^2,(p+q)^2) &= m_b^2 f_K \int_0^1 \frac{du}{m_b^2 - (q+up)^2}\bigg\{\varphi_K(u) + \frac{\mu_K}{m_b} u\phi^p_{3K}(u) + \frac{\mu_K}{6m_b}\bigg[2 + \frac{m_b^2 + q^2 - u^2p^2}{m_b^2 - (q+up)^2}\bigg]\phi^\sigma_{3K}(u) \\ &- \frac{m_b^2\phi_{4K}(u)}{2(m_b^2 - (q+up)^2)^2} - \frac{u}{m_b^2 - (q+up)^2}\int_0^u dv\psi_{4K}(v)\bigg\} + \int_0^1 dv \int \frac{\mathcal{D}\alpha}{[m_b^2 - (q+Xp)^2]^2} \\ &\times\bigg\{m_b f_{3K}(4v(q\cdot p) - (1-2v)Xp^2)\Phi_{3K}(\alpha_i) + m_b^2 f_K\bigg[3(\Psi_{4K}(\alpha_i) + \tilde{\Psi}_{4K}(\alpha_i)) \\ &+ \frac{4v(1-v)(q\cdot p + Xp^2)}{m_b^2 - (q+Xp)^2}\Xi_{4K}(\alpha_i) - \bigg(1 - \frac{Xp^2}{q\cdot p + Xp^2}\bigg)(\Psi_{4K}(\alpha_i) + \Phi_{4K}(\alpha_i) + \tilde{\Psi}_{4K}(\alpha_i) \\ &+ \tilde{\Phi}_{4K}(\alpha_i))\bigg]\bigg\} - m_b^2 f_K \int_0^1 dv \int \mathcal{D}\alpha \int_0^X d\xi \frac{1}{[m_b^2 - (q+(X-\xi)p)^2]^2}\frac{p^2 q\cdot p}{(q\cdot p + (X-\xi)p^2)^2} \\ &\times(\Psi_{4K}(\alpha_i) + \Phi_{4K}(\alpha_i) + \tilde{\Psi}_{4K}(\alpha_i) + \tilde{\Phi}_{4K}(\alpha_i)),\end{aligned} \quad (10)$$

$$\begin{aligned}\tilde{F}_0(q^2,(p+q)^2) &= m_b f_K \int_0^1 \frac{du}{m_b^2 - (q+up)^2}\{\mu_K\phi^p_{3K}(u) + \frac{\mu_K}{6}\bigg[1 - \frac{m_b^2 - q^2 + u^2p^2}{m_b^2 - (q+up)^2}\bigg]\frac{\phi^\sigma_{3K}(u)}{u} \\ &- \frac{m_b}{m_b^2 - (q+up)^2}\int_0^u dv\psi_{4K}(v)\bigg\} + m_b f_{3K}\int_0^1 dv \int \frac{\mathcal{D}\alpha}{[m_b^2 - (q+Xp)^2]^2}(2v-3)p^2\Phi_{3K}(\alpha_i) \\ &+ 4m_b^2 f_K \int_0^1 dv \int \mathcal{D}\alpha \int_0^X d\xi \frac{1}{[m_b^2 - (q+(X-\xi)p)^2]^3}p^2(\Psi_{4K}(\alpha_i) + \Phi_{4K}(\alpha_i) + \tilde{\Psi}_{4K}(\alpha_i) \\ &+ \tilde{\Phi}_{4K}(\alpha_i)),\end{aligned} \quad (11)$$

$$F_0^T(q^2,(p+q)^2) = m_b f_K \int_0^1 \frac{du}{m_b^2-(q+up)^2}\left\{\varphi_K(u) + \frac{m_b\mu_K}{3(m_b^2-(q+up)^2)}\phi_{3K}^\sigma(u) - \frac{1}{2(m_b^2-(q+up)^2)}\left(\frac{1}{2}+\frac{m_b^2}{m_b^2-(q+up)^2}\right)\phi_{4K}(u)\right\} + m_b f_K\int_0^1 dv \int \frac{\mathcal{D}\alpha}{[m_b^2-(q+Xp)^2]^2} \\ + \left\{2\Psi_{4K}(\alpha_i) - (1-2v)\Phi_{4K}(\alpha_i) + 2(1-2v)\tilde{\Psi}_{4K}(\alpha_i) - \tilde{\Phi}_{4K}(\alpha_i) \\ + \frac{4v(1-v)(q\cdot p + Xp^2)}{m_b^2-(q+Xp)^2}\Xi_{4K}(\alpha_i)\right\}, \tag{12}$$

respectively, with $X = \alpha_1 + v\alpha_3$, $\mathcal{D}\alpha = d\alpha_1 d\alpha_2 d\alpha_3 \delta(1-\alpha_1-\alpha_2-\alpha_3)$, and with the definitions of the twist-2 (φ_K), twist-3 (ϕ_{3K}^p, ϕ_{3K}^σ, Φ_{3K}), and twist-4 (ϕ_{4K}, ψ_{4K}, Φ_{4K}, Ψ_{4K}, $\tilde{\Phi}_{4K}$, $\tilde{\Psi}_{4K}$) kaon DA's from [19]. It is easy to see that for $p^2 = 0$ the above expressions resemble those given in [14] for the $B \to \pi$ form factors. Here we have also included a contribution from an additional G-parity breaking twist-4 three-particle DA, Ξ_{4K}, which was first introduced in [24]. Its parameter, as well as the rest of DA parameters, are taken from [19] where the renormalon model is used for describing SU(3)-symmetry breaking for twist-4 DAs. For all details about the SU(3)-symmetry breaking effects in the kaon DAs the reader is advised to see [19].

The massless (m_K^2, $m_s \to 0$) NLO contributions to the LCSR expressions for $B \to K$ form factors, $F_1(p,(p+q)^2)$, etc., are the same as those given in the appendix of [14] for $B \to \pi$ form factors. All features of these $O(\alpha_s)$ corrections are already listed in [14], and we will not repeat them in this paper. Unfortunately, we were not able to perform the full NLO calculation with the mass effects included. The problem appeared by inclusion of the chirally noninvariant piece of the s-quark propagator, being proportional to m_s, in the calculation of diagrams from Fig. 2. Since now $p^2 = m_K^2$, the IR divergences were not present, but there appeared additional UV divergences proportional to m_s, which have clearly exhibited the mixing among different twists. We could not achieve the cancellation of such singularities, since obviously some additional ingredient of mass mixing among twist-2 and twist-3 contributions was missing. Although interesting *per se*, these mixing effects are nontrivial, and there are beyond a scope of this paper. Hence, the repercussions of the mass effects at NLO could only be analyzed by setting $m_s \to 0$. We are aware that keeping $O(m_K^2)$ effects, and neglecting the same order effect of m_s-proportional terms is not completely justified; therefore, we have used the result with $p^2 = m_K^2$ corrections only as an estimation for the neglected mass effects at NLO.

The final LCSR expressions for $B_{(s)} \to K$ form factors, with the $p^2 = m_K^2$ corrections included, have a similar form as those for the $p^2 = 0$ shown in [14], but with a more complicated structure now. Therefore we are not going to present them here.[1]

III. DIRECT INTEGRATION OF THE LCSR EXPRESSIONS

The sum rule expression for the form factors (9) requires, by definition, calculation of the imaginary part of hard-scattering amplitudes. Complexity of the extraction of imaginary parts of sum rule amplitudes arises already at the LO level, as one can notice from the expressions in Appendix A. One has to be particularly careful about the appearance of the surface terms there. At the NLO the results are far more complicated, as one can see in Appendix B of [14]. The inclusion of $p^2 = m_K^2$ effects at NLO makes the calculation even more involved.

Therefore, we would like to present here a method which completely avoids the use of explicit imaginary parts of hard-scattering amplitudes, allowing one to numerically calculate amplitudes of LCSRs, analytically continuing integrands to the complex plane. While this method was used as a check in [14], here we would like to emphasis its features and possible advantages over the traditional way of calculating sum rule amplitudes, especially when one performs NLO calculations.

The main idea of the method is to deform the path of integration in order to avoid poles which are located near real axes. Because of the Cauchy theorem, the deformation is legitimate if the integrand is an analytic function inside the region bounded by the original and the new path of integration. To check the analyticity of the integrand we have to examine its pole structure. In the case of NLO calculations, it is also necessary to examine the position of cuts in logarithms and dilogarithms. Fortunately, there are just a few characteristic structures which have to be investigated.

At LO, Eqs. (10)–(12), there are two possibilities to hit the pole, when

$$m_b^2 - (q+ap)^2 = 0, \quad \text{or} \quad q\cdot p + ap^2 = 0, \tag{13}$$

[1] Interested readers can obtain all expressions from the authors in *Mathematica* [25] form.

condition is fulfilled. In above, $a = u, X, X - \xi$ represents fraction of momenta between 0 and 1, over which it has to be integrated. For further considerations, it is convenient to introduce the notations

$$r_1 = \frac{q^2}{m_b^2}, \qquad r_2 = \frac{s}{m_b^2}, \qquad r_3 = \frac{p^2}{m_b^2} = \frac{m_K^2}{m_b^2}, \qquad (14)$$
$$\rho = (1-a)r_1 + ar_2 - a(1-a)r_3.$$

By using (14), the conditions from (13) can be written as

$$m_b^2(1-\rho) = 0, \quad \text{or} \quad \frac{m_b^2}{2}(r_2 - r_1 - r_3(1-2a)) = 0. \qquad (15)$$

In the case of interest $r_2 > r_1 + r_3 > 0$, the second condition from above cannot be fulfilled and therefore there is no pole for $q \cdot p + ap^2 = 0$. From the first condition in (15), it follows that the integrand is approaching a pole when $\rho \to 1$. That happens for the real values of r_2 and a in the integration range. Note that in Eqs. (10)–(13) we have omitted an infinitesimal imaginary quantity $i\epsilon$ which appears in Feynman propagators. Taking it into account, the exact position of the pole is given by the equation $1 - \rho - i\epsilon = 0$, which means that the poles are not located on the real axes of r_2, but slightly below. As a consequence, one can deform the r_2 path of integration into the upper half of the r_2 complex plane to avoid passing near the poles. If poles are far away from the integration path, the integration is numerically completely stabile. The problem remains only when the poles coincide with the end points of the integration. For the integration over r_2, the end points are at 1 and $s_0^{B_{(s)}}/m_b^2$. Then ρ becomes

$$\rho = a + (1-a)r_1 - a(1-a)r_3 \quad \text{for } r_2 = 1, \qquad (16)$$

$$\rho = a\frac{s_0}{m_b^2} + (1-a)r_1 - a(1-a)r_3 \quad \text{for } r_2 = \frac{s_0^{B_{(s)}}}{m_b^2} > 1. \qquad (17)$$

In both cases ρ can be equal to 1 in the range of integration over a. In the case (16), ρ is equal to 1 for $a = 1$, which is the worst possible case because this pole is located at the end point of two integrations. In (17), $\rho = 1$ for $0 < a < 1$, where, due to the specific values of r_1, r_3, and s_0, a cannot be near 0 or 1. However, in both cases it is possible to move away from the poles. The complete procedure is going in this way. The first step is to shift the lower limit of r_2 (i.e., s) integration to any point between $r_1 + r_3 < r_2 < 1$. That is legitimate because all integrands are real for $r_2 < 1$ and we are interested only in an imaginary part of the integrand, as can be seen from (9). The lower limit $r_1 + r_3$ is necessary to evade the possibility to fulfill the second condition from Eq. (15). Now we move the operation of taking the imaginary part in (9) outside the integral. As the third step we deform the path of the r_2 integration into the upper half of the complex r_2-plane, so that all poles are away from the integration region. For the calculation presented here, the new integration path is the semicircle in the complex r_2-plane; see Fig. 3. As mentioned before, the pole condition still can be satisfied at the end points of integration. However, since the lower end point of the r_2 integration is now <1, the pole condition ($\rho = 1$) cannot be fulfilled at that end point. For the upper end point ($r_2 = s_0^{B_{(s)}}/m_b^2$) the situation is as presented by Eq. (17). Because of the fact that this pole is in the middle of the range of a integration, it is possible to avoid it now by deforming the contour of a-integration into the upper half of the complex a-plane. Here, we again deform the integration path in the shape of the semicircle, as shown in Fig. 3. After that, all poles are away from the integration regions and all integrals can be performed numerically without facing instabilities in the integration. At the end, it remains to take the imaginary part to get the final result.

For the NLO calculation, in addition, one has to check analytical properties of appearing logarithms and polylogarithms. It happens that for the case of the interest in one of the logarithms it is impossible to avoid crossing the cut when both variables r_2 and a are continued to the upper

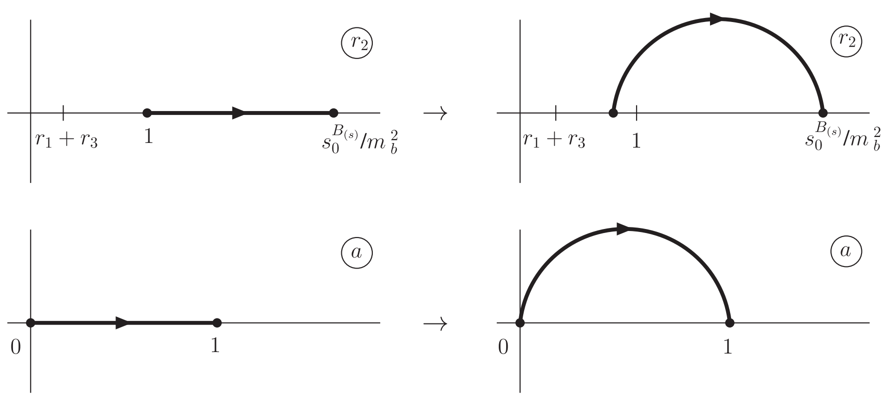

FIG. 3. Replacing the integration intervals by the contours in the complex planes of $a = u, X, X - \xi$, and $r2 = s/m_b^2$ variables in the procedure of numerical integration of LCSR amplitudes.

half of the complex space. To avoid crossing the cut, we have continued only r_2 to the complex plane. But now, the path of the integration for the variable a will pass near the pole when r_2 is approaching the end point $s_0^{B_{(s)}}/m_b^2$. Although the problem can be cured by the variable transformation and a sophisticated analytical continuation, considering the precision needed for the calculation, such a sophisticated method is obsolete indeed. The numerical instability shows up in the third significant digit, and therefore does not affect the final numerical results.

IV. UPDATED PREDICTIONS FOR THE $B_{(s)} \to K$ FORM FACTORS

All input parameters are listed in Appendix B. It is a compilation of the most recent determination of parameters entering the calculation.

The renormalization scale is given by the expression $\mu_{(s)} = \sqrt{m_{B_{(s)}}^2 - m_b^2}$. Therefore, for the $f_{BK}^{0,+,T}$ form factors we use $\mu = 3$ GeV and for $f_{B_sK}^{0,+,T}$ the renormalization scale is $\mu_s = 3.4$ GeV. As usual, we will check the sensitivity of the results on the variation of above scales and will include it in the error estimation.

From the general LCSR expressions for the form factors, (5)–(7), one can note that the decay constant f_B (and correspondingly f_{B_s} for $B_s \to K$ decays) enters the calculation. To reduce the dependence of the form factors on the input parameters, we replace f_B and f_{B_s} by two-point sum rule expressions in the $\overline{MS}$ scheme from [15] to $O(\alpha_s, m_s^2)$ accuracy and calculate them for our preferred values of parameters.

The usual method for deriving the working region of Borel parameters and determining effective threshold parameters is used. We investigate the behavior of the perturbative expansion and smallness of the continuum contribution (to be less then 30% of the total contribution), and require that the derivative over the Borel parameter of the expression for a particular decay constant, which gives the sum rule for m_B^2 ($m_{B_s}^2$), does not deviate more than 0.5–1% from the experimental values for those masses. We obtain the following sets of parameters: $\bar{M}^2 = 5 \pm 1$ GeV^2 and $\bar{s}_0^B = 35.6^{-0.9}_{+2.1}$ GeV^2 for the B-meson decay constant f_B calculated at $\mu = 3$ GeV, and $\bar{M}_s^2 = 6.1 \pm 1.5$ GeV^2 and $\bar{s}_0^{B_s} = 36.6^{-1.6}_{+1.9}$ GeV^2 for f_{B_s} calculated at $\mu_s = 3.4$ GeV. Note that the calculated central values of $\bar{s}_0^{B_{(s)}}$ follow the naive relation $\bar{s}_0^{B_s} - \bar{s}_0^B \simeq m_{B_s}^2 - m_B^2 \simeq 1$ GeV^2. Employing these values, the resulting decay constants are

$$f_B = 214 \pm 18 \text{ MeV}, \qquad f_{B_s} = 250 \pm 20 \text{ MeV}. \quad (18)$$

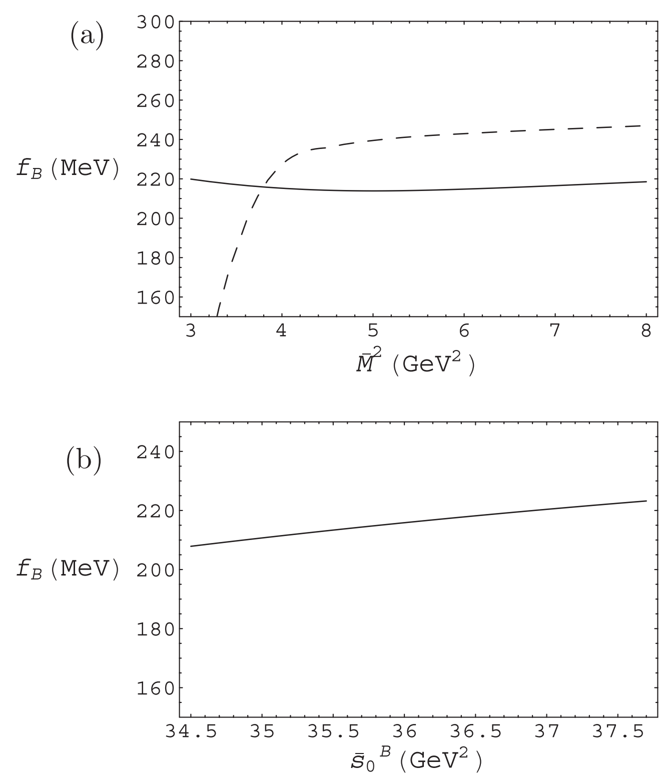

FIG. 4. Dependence of f_B on (a) the Borel parameter $\bar{M}^2$ shown for $\mu = 3$ GeV (solid line) and $\mu = 6$ GeV (dashed line) and (b) the effective threshold parameter $\bar{s}_0^B$ using the central values of all other input parameters.

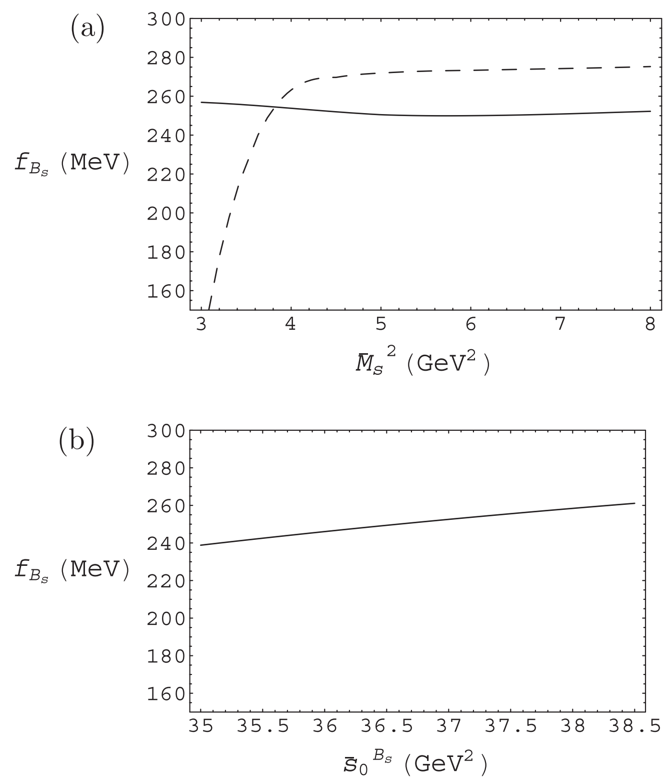

FIG. 5. Dependence of f_{B_s} on (a) the Borel parameter $\bar{M}_s^2$ shown for $\mu = 3.4$ GeV (solid line) and $\mu = 6$ GeV (dashed line) and (b) the effective threshold parameter $\bar{s}_0^{B_s}$ using the central values of all other input parameters.

In the LCSR expression for the form factors some of the uncertainties are going to cancel in the ratios, and therefore the error intervals of the f_B and f_{B_s} input will reduce, as one can see from the following numbers, $f_B = 214 \pm 9$ MeV and $f_{B_s} = 250 \pm 11$ MeV, where the calculated error intervals come from the variation of $\bar{s}_0^{B_{(s)}}$ and $\bar{M}^2_{(s)}$ only. The dependence of the decay constants on $\bar{M}^2_{(s)}$ and $\bar{s}_0^{B_{(s)}}$ appears to be mild, as shown in Figs. 4 and 5. The SU(3) violation among decay constants is [15]

$$\frac{f_{B_s}}{f_B} = 1.16 \pm 0.05, \tag{19}$$

which nicely agrees with the values obtained from the lattice calculation and by different quark models [26–28].

The method of extraction of the Borel parameters M and M_s, and the effective thresholds s_0^B and $s_0^{B_s}$ for $f^{+,0,T}_{B_{(s)}K}$ form factors is similar to the above, and it is the same as described in [14]. We require that the subleading twist-4 terms in the LO are small, less than 3% of the LO twist-2 term, that the NLO corrections of twist-2 and twist-3 parts are not exceeding 30% of their LO counterparts, and that the subtracted continuum remains small, which fixes the allowed range of $M^2_{(s)}$. The effective threshold parameters are again fitted so that the derivative over $-1/M^2_{(s)}$ of the expression of the complete LCSRs for a particular form factor reproduces the physical masses $m^2_{B_{(s)}}$ with a high accuracy of $O(0.5\%–1\%)$ in the stability region of the sum rules. These demands provide us the following central values for the sum rule parameters: $M^2 = 18\ \text{GeV}^2$, $s_0^B = 38\ \text{GeV}^2$, $M_s^2 = 19\ \text{GeV}^2$, and $s_0^{B_s} = 39\ \text{GeV}^2$. The dependence of the form factors on the these parameters is depicted in Figs. 6 and 7.

The complete numerical analysis yields the following predictions for the vector $B \to K$ and $B_s \to K$ form factors at zero momentum transfer:

$$f^+_{BK}(0) = 0.368 \pm 0.011|_{a_1,a_2} \pm 0.008|_{M,\bar{M}} \begin{array}{l}+0.017\\-0.008\end{array}\Big|_{\mu} \pm 0.006|_{m_b} \begin{array}{l}+0.036\\-0.024\end{array}\Big|_{\mu_\pi} +0.026|_{m_K^2 \text{ at NLO}}, \tag{20}$$

$$f^+_{B_sK}(0) = 0.300 \pm 0.007|_{a_1,a_2} \begin{array}{l}+0.006\\-0.007\end{array}\Big|_{M_s,\bar{M}_s} \begin{array}{l}+0.004\\-0.003\end{array}\Big|_{\mu} \begin{array}{l}+0.001\\-0.002\end{array}\Big|_{m_b} \begin{array}{l}+0.034\\-0.020\end{array}\Big|_{\mu_\pi} +0.026|_{m_K^2 \text{ at NLO}}, \tag{21}$$

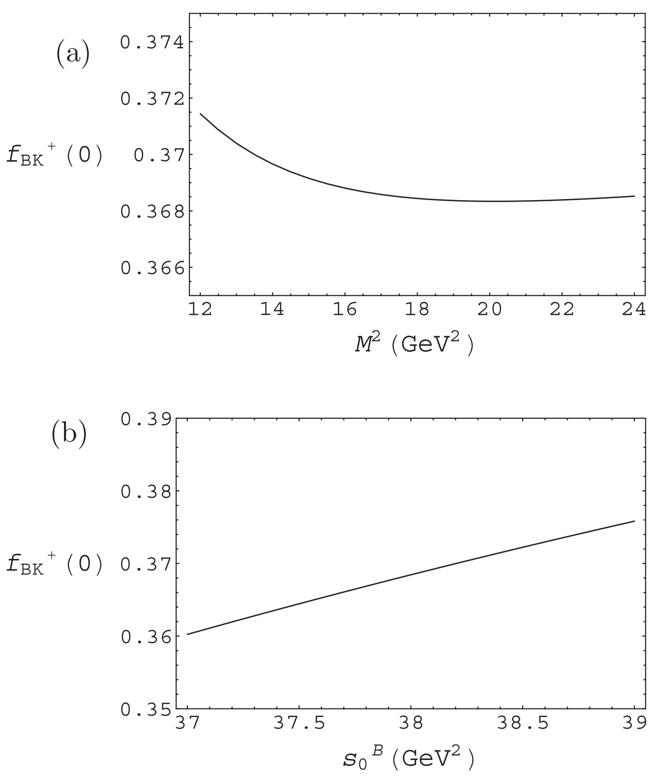

FIG. 6. Dependence of f^+_{BK} on (a) the Borel parameter M^2 and (b) the effective threshold parameter s_0^B using the central values of all other input parameters.

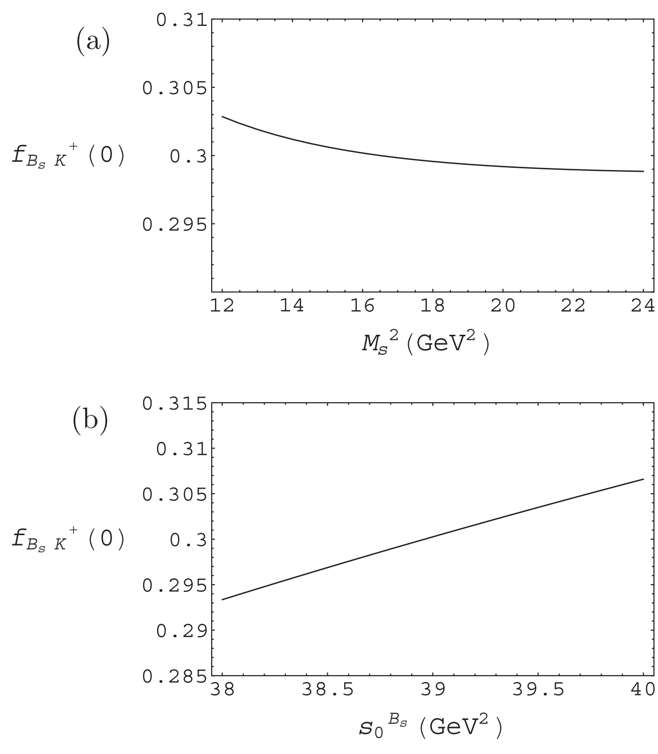

FIG. 7. Dependence of $f^+_{B_sK}$ on (a) the Borel parameter M_s^2 and (b) the effective threshold parameter $s_0^{B_s}$ using the central values of all other input parameters.

where the central value for f^+_{BK} is calculated at $\mu = 3.0$ GeV, $M^2 = 18.0$ GeV^2, $s_0^B = 38$ GeV^2, $\bar{M}^2 = 5.0$ GeV^2, and $\bar{s}_0^B = 35.6$ GeV^2, and for $f^+_{B_sK}$ at $\mu_s = 3.4$ GeV, $M_s^2 = 19.0$ GeV^2, $s_0^{B_s} = 39$ GeV^2, $\bar{M}_s^2 = 6.1$ GeV^2, $\bar{s}_0^{B_s} = 36.6$ GeV^2. The central values for the parameters of the twist-2 kaon DA are $a_1^K(1\text{ GeV}) = 0.10$ and $a_2^K(1\text{ GeV}) = 0.25$. The last error in (20) and (21) comes from the neglected $O(m_K^2)$ effects at NLO.

Finally, adding all uncertainties in quadratures, and to be on the safe side, allowing that the real mass corrections at NLO could reduce the final result, we obtain the following values for different $B \to K$ form factors:

$$f^+_{BK}(0) = f^0_{BK}(0) = 0.36^{+0.05}_{-0.04}, \tag{22}$$

$$f^T_{BK}(0) = 0.38 \pm 0.05, \tag{23}$$

and for $B_s \to K$ form factors,

$$f^+_{B_sK}(0) = f^0_{B_sK}(0) = 0.30^{+0.04}_{-0.03}, \tag{24}$$

$$f^T_{B_sK}(0) = 0.30 \pm 0.05. \tag{25}$$

Their q dependence is shown in Figs. 8 and 9, where the values in the allowed LCSR kinematical regime are shown. The above results for the form factors are in an overall agreement with those extracted by other methods [27–29]. The predictions include also the uncertainty from the inclusion of m_K^2 effects at NLO, which is relatively large, as can be deduced from (20) and (21). However, one has to be aware that this error only gives us a flavor of the size of neglected mass corrections at NLO, since the m_s effects in the hard-scattering amplitude could not be included, and we expect that there will be a partial cancellation among m_s and m_K^2 contributions, being of similar size. At the leading order, the inclusion of m_s effects (appearing only in DAs) and m_K^2 effects reduces the results by 2.5%–4%, depending of the value of q^2.

In order to be able to comment on the SU(3)-breaking effects, these values have to be compared with the results

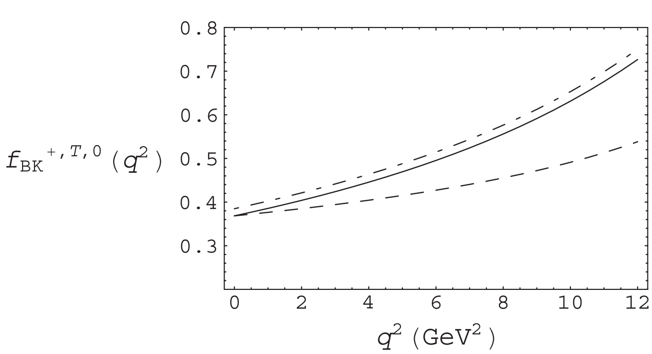

FIG. 8. The LCSR prediction for form factors $f^+_{BK}(q^2)$ (solid line), $f^0_{BK}(q^2)$ (dashed line), and $f^T_{BK}(q^2)$ (dash-dotted line) at $0 < q^2 < 12$ GeV^2 and for $\mu = 3$ GeV, $s_0^B = 38$ GeV^2, $M^2 = 18$ GeV^2, and the central values of all other input parameters.

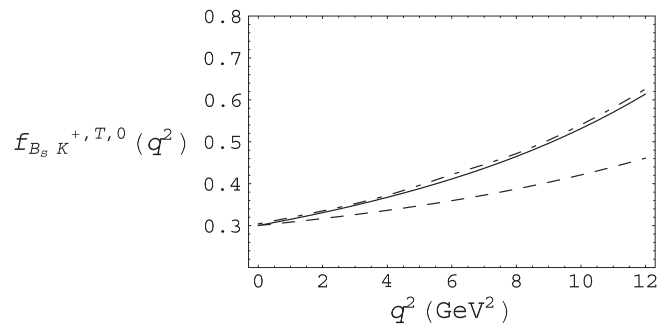

FIG. 9. The LCSR prediction for form factors $f^+_{B_sK}(q^2)$ (solid line), $f^0_{B_sK}(q^2)$ (dashed line), and $f^T_{B_sK}(q^2)$ (dash-dotted line) at $0 < q^2 < 12$ GeV^2 and for $\mu = 3.4$ GeV, $s_0^{B_s} = 39$ GeV^2, $M_s^2 = 19$ GeV^2, and the central values of all other input parameters.

obtained by the same method for $B \to \pi$ form factors [14], which we quote here:

$$f^+_{B\pi}(0) = f^0_{B\pi}(0) = 0.26^{+0.04}_{-0.03}, \tag{26}$$

$$f^T_{B\pi}(0) = 0.255 \pm 0.035. \tag{27}$$

By varying parameters in a correlated way, finally we predict the following SU(3)-breaking ratios:

$$\frac{f^+_{BK}(0)}{f^+_{B\pi}(0)} = 1.38^{+0.11}_{-0.10}, \qquad \frac{f^+_{B_sK}(0)}{f^+_{B\pi}(0)} = 1.15^{+0.17}_{-0.09}, \tag{28}$$

$$\frac{f^T_{BK}(0)}{f^T_{B\pi}(0)} = 1.49^{+0.18}_{-0.06}, \qquad \frac{f^T_{B_sK}(0)}{f^T_{B\pi}(0)} = 1.17^{+0.15}_{-0.11}. \tag{29}$$

The complete SU(3) violation comes from SU(3)-breaking corrections in all parameters, mainly from f_K/f_π, μ_K/μ_π, from the difference in the sum rule parameters, s_B and M, as well as from the difference in the f_{B_s} and f_B ratio.

Compared with the values from the second paper in [17], where the similar LCSR analysis was done, we find nice agreement with the results in (28).

It is also interesting to explore an overall SU(3)-breaking factor, which appears in factorization models for $B_{(s)} \to K\pi$ amplitudes [16,30]:

$$\xi = \frac{f_K}{f_\pi}\frac{f^+_{B\pi}(m_K^2)}{f^+_{B_sK}(m_\pi^2)}\frac{m_B^2 - m_\pi^2}{m_{B_s}^2 - m_K^2} = 1.01^{+0.07}_{-0.15}. \tag{30}$$

For the f_K/f_π ratio we use (B3). Although there is a SU(3) violation among form factors and in the masses, the predicted value for ξ shows almost exact SU(3) symmetry. On the other hand, the above ratio enters the prediction for $B_s \to K^-\pi^+$ amplitude obtained by employing U-spin symmetry. U-spin symmetry cannot be trusted [17], as we can note by inspecting another U-spin relation. By neglecting penguin and annihilation contributions, under the U-spin symmetry assumption $A_{\text{fact}}(B_s \to K^+K^-)/A_{\text{fact}}(B_d \to \pi^+\pi^-) \sim 1$, [17,30,31], while our prediction amounts to

$$\frac{A_{\rm fact}(B_s \to K^+K^-)}{A_{\rm fact}(B_d \to \pi^+\pi^-)} = \frac{f_K}{f_\pi}\frac{f^+_{B_sK}(m_K^2)}{f^+_{B\pi}(m_\pi^2)}\frac{m_{B_s}^2 - m_K^2}{m_B^2 - m_\pi^2} = 1.41^{+0.20}_{-0.11}, \tag{31}$$

a quite substantial U-spin violation.

V. SUMMARY

In this paper we have investigated the SU(3)-symmetry breaking effects in the $B \to K$ and $B_s \to K$ form factors. The analysis has involved the SU(3)-breaking corrections both in the LO (up to twist-4 corrections), as well as in the NLO calculation, estimating SU(3) corrections for the twist-2 and twist-3 contributions. Although at NLO we were not able to consistently include $O(m_s) \sim O(m_K^2)$ effects, we have included m_K^2 effects in the error analysis of our results. We have presented a method of numerical integration of sum rule amplitudes, which greatly facilitates the calculation, especially the calculation of the radiative corrections. By investigating some of the SU(3) and U-spin symmetry relations, we have shown that such relations have to be considered with a precaution, since some of them can be badly broken.

ACKNOWLEDGMENTS

We are grateful to A. Khodjamirian, A. Lenz, and K. Passek-Kumerički for useful discussions. The work is supported by the Ministry of Science, Education, and Sport of the Republic of Croatia, under Contract No. 098-0982930-2864 and by the Alexander von Humboldt Foundation.

APPENDIX A: EXPLICIT FORMULAS FOR THE LEADING-ORDER LCSR EXPRESSIONS

Although the intention of this paper is to promote the numerical method for calculating LCSR amplitudes, for which the explicit expressions for the imaginary parts are superfluous, because the result can be obtained by direct integration of the starting amplitudes (at LO they are given by Eqs. (10)–(12)), we have decided to list here the LO LCSR expressions for $f_{B_{(s)}K}$ form factors, since to our best knowledge, these expressions were never clearly presented in a form which includes complete mass corrections.

The LO part of the f^+_{BK} LCSR, (5), has the following form:

$$\begin{aligned}
F_0(q^2, M^2, s_0^B) = {}& m_b^2 f_K \int_{u_0}^1 du\, e^{-(m_b^2 - q^2\bar{u} + m_K^2 u\bar{u})/uM^2}\Bigg\{\frac{\varphi_K(u)}{u} + \frac{\mu_K}{m_b}\Bigg[\phi^p_{3K}(u) + \frac{1}{6}\Bigg(2\frac{\phi^\sigma_{3K}(u)}{u} - \frac{1}{m_b^2 - q^2 + u^2 m_K^2} \\
&\times\Bigg((m_b^2 + q^2 - u^2 m_K^2)\frac{d\phi^\sigma_{3K}(u)}{du} - \frac{4u m_K^2 m_b^2}{m_b^2 - q^2 + u^2 m_K^2}\phi^\sigma_{3K}(u)\Bigg)\Bigg)\Bigg] \\
&+ \frac{1}{m_b^2 - q^2 + u^2 m_K^2}\Bigg[u\psi_{4K}(u) + \Bigg(1 - \frac{2u^2 m_K^2}{m_b^2 - q^2 + u^2 m_K^2}\Bigg)\int_0^u dv\,\psi_{4K}(v) \\
&- \frac{m_b^2}{4}\frac{u}{m_b^2 - q^2 + u^2 m_K^2}\Bigg(\frac{d^2}{du^2} - \frac{6u m_K^2}{m_b^2 - q^2 + u^2 m_K^2}\frac{d}{du} + \frac{12 u m_K^4}{(m_b^2 - q^2 + u^2 m_K^2)^2}\Bigg)\phi_{4K}(u) \\
&- \Bigg(\frac{d}{du} - \frac{2u m_K^2}{m_b^2 - q^2 + u^2 m_K^2}\Bigg)\Bigg(\Bigg(\frac{f_{3K}}{m_b f_K}\Bigg)I_{3K}(u) + I_{4K}(u) - \frac{dI^{\Xi}_{4K}(u)}{du}\Bigg) \\
&- \frac{2u m_K^2}{m_b^2 - q^2 + u^2 m_K^2}\Bigg(u\frac{d}{du} + \Bigg(1 - \frac{4u^2 m_K^2}{m_b^2 - q^2 + u^2 m_K^2}\Bigg)\Bigg)\bar{I}_{4K}(u) \\
&+ \frac{2u m_K^2(m_b^2 - q^2 - u^2 m_K^2)}{(m_b^2 - q^2 + u^2 m_K^2)^2}\Bigg(\frac{d}{du} - \frac{6u m_K^2}{m_b^2 - q^2 + u^2 m_K^2}\Bigg)\int_u^1 d\xi\,\bar{I}_{4K}(\xi)\Bigg]\Bigg\} \\
&+ \frac{m_b^2 f_K e^{-m_b^2/M^2}}{m_b^2 - q^2 + m_K^2}\Bigg[-\int_0^1 dv\,\psi^{WW}_{4K}(v) + \frac{m_b^2}{4}\frac{1}{m_b^2 - q^2 + m_K^2}\Bigg(\frac{d\phi^{WW}_{4K}(u)}{du}\Bigg)_{u\to 1}\Bigg],
\end{aligned} \tag{A1}$$

where $\bar{u} = 1 - u$, $u_0 = (q^2 - s_0^B + m_K^2 + \sqrt{(q^2 - s_0^B + m_K^2)^2 - 4m_K^2(q^2 - m_b^2)})/(2m_K^2)$, and the short-hand notations introduced for the integrals over three-particle DA's are

$$\begin{aligned} I_{3K}(u) &= \int_0^u d\alpha_1 \int_{(u-\alpha_1)/(1-\alpha_1)}^1 \frac{dv}{v}[4vp\cdot q - (1-2v)um_K^2]\Phi_{3K}(\alpha_i)\Big|_{\alpha_2=1-\alpha_1-\alpha_3,\alpha_3=(u-\alpha_1)/v}, \\ I_{4K}(u) &= \int_0^u d\alpha_1 \int_{(u-\alpha_1)/(1-\alpha_1)}^1 \frac{dv}{v}[2\Psi_{4K}(\alpha_i) - \Phi_{4K}(\alpha_i) + 2\tilde{\Psi}_{4K}(\alpha_i) - \tilde{\Phi}_{4K}(\alpha_i)]\Big|_{\alpha_2=1-\alpha_1-\alpha_3,\alpha_3=(u-\alpha_1)/v}, \\ \bar{I}_{4K}(u) &= \int_0^u d\alpha_1 \int_{(u-\alpha_1)/(1-\alpha_1)}^1 \frac{dv}{v}[\Psi_{4K}(\alpha_i) + \Phi_{4K}(\alpha_i) + \tilde{\Psi}_{4K}(\alpha_i) + \tilde{\Phi}_{4K}(\alpha_i)]\Big|_{\alpha_2=1-\alpha_1-\alpha_3,\alpha_3=(u-\alpha_1)/v}, \\ I_{4K}^{\Xi}(u) &= \int_0^u d\alpha_1 \int_{(u-\alpha_1)/(1-\alpha_1)}^1 \frac{dv}{v}[v(1-v)\Xi_{4K}(\alpha_i)]\Big|_{\alpha_2=1-\alpha_1-\alpha_3,\alpha_3=(u-\alpha_1)/v}. \end{aligned} \tag{A2}$$

The twist-4 two-particle DAs are defined with the help of the two DAs [19]: $\phi_{4K} = \phi_{4K}^{T4} + \phi_{4K}^{WW}$ and $\psi_{4K} = \psi_{4K}^{T4} + \psi_{4K}^{WW}$. The leading-order LCSR for $f_{BK}^+ + f_{BK}^-$, (6), looks like

$$\begin{aligned} \tilde{F}_0(q^2, M^2, s_0^B) = m_b^2 f_K \int_{u_0}^1 du e^{-(m_b^2 - q^2\bar{u} + m_K^2 u\bar{u})/(uM^2)} \Bigg\{ &\frac{\mu_K}{m_b}\left(\frac{\phi_{3K}^p(u)}{u} + \frac{1}{6u}\frac{d\phi_{3K}^\sigma(u)}{du}\right) \\ &+ \frac{1}{m_b^2 - q^2 + u^2 m_K^2}\Bigg[\psi_{4K}(u) - \frac{2um_K^2}{m_b^2 - q^2 + u^2m_K^2}\int_0^u dv\psi_{4K}(v) \\ &+ m_K^2\left(\frac{d}{du} - \frac{2um_K^2}{m_b^2 - q^2 + u^2m_K^2}\right)\left(\frac{f_{3K}}{f_K m_b}\right)\tilde{I}_{3K}(u) + \frac{2um_K^2}{m_b^2 - q^2 + u^2m_K^2}\left(\frac{d^2}{du^2} - \frac{6um_K^2}{m_b^2 - q^2 + u^2m_K^2}\frac{d}{du}\right. \\ &\left.+ \frac{12u^2m_K^4}{(m_b^2 - q^2 + u^2m_K^2)^2}\right)\int_u^1 d\xi \bar{I}_{4K}(\xi)\Bigg]\Bigg\} + \frac{m_b^2 f_K e^{-m_b^2/M^2}}{m_b^2 - q^2 + m_K^2}\left[-\int_0^1 dv\psi_{4K}^{WW}(v)\right], \end{aligned} \tag{A3}$$

where

$$\tilde{I}_{3K}(u) = \int_0^u d\alpha_1 \int_{(u-\alpha_1)/(1-\alpha_1)}^1 \frac{dv}{v}[(3-2v)]\Phi_{3K}(\alpha_i)\Big|_{\alpha_2=1-\alpha_1-\alpha_3,\alpha_3=(u-\alpha_1)/v}. \tag{A4}$$

Finally, the leading-order LCSR for the penguin form factor, (7), reads

$$\begin{aligned} F_0^T(q^2, M^2, s_0^B) = m_b f_K \int_{u_0}^1 du e^{-(m_b^2 - q^2\bar{u} + m_K^2 u\bar{u})/uM^2} \Bigg\{ &\frac{\varphi_K(u)}{u} - \frac{m_b\mu_K}{3(m_b^2 - q^2 + u^2m_K^2)} \\ &\times\left(\frac{d\phi_{3K}^\sigma(u)}{du} - \frac{2um_K^2}{m_b^2 - q^2 + u^2m_K^2}\phi_{3K}^\sigma(u)\right) + \frac{1}{m_b^2 - q^2 + u^2m_K^2}\Bigg[\left(\frac{d}{du} - \frac{2um_K^2}{m_b^2 - q^2 + u^2m_K^2}\right) \\ &\times\left(\frac{1}{4}\phi_{4K}(u) - I_{4K}^T(u) + \frac{dI_{4K}^{\Xi}(u)}{du}\right) - \frac{m_b^2 u}{4(m_b^2 - q^2 + u^2m_K^2)}\left(\frac{d^2}{du^2} - \frac{6um_K^2}{m_b^2 - q^2 + u^2m_K^2}\frac{d}{du}\right. \\ &\left.+ \frac{12um_K^4}{(m_b^2 - q^2 + u^2m_K^2)^2}\right)\phi_{4K}(u)\Bigg]\Bigg\} + \frac{m_b f_K e^{-m_b^2/M^2}}{m_b^2 - q^2 + m_K^2}\left[\frac{m_b^2}{4}\frac{1}{m_b^2 - q^2 + m_K^2}\left(\frac{d\phi_{4K}^{WW}(u)}{du}\right)_{u\to 1}\right] \end{aligned} \tag{A5}$$

and

$$I_{4K}^T(u) = \int_0^u d\alpha_1 \int_{(u-\alpha_1)/(1-\alpha_1)}^1 \frac{dv}{v}[2\Psi_{4K}(\alpha_i) - (1-2v)\Phi_{4K}(\alpha_i) + 2(1-2v)\tilde{\Psi}_{4K}(\alpha_i) - \tilde{\Phi}_{4K}(\alpha_i)]\Big|_{\alpha_2=1-\alpha_1-\alpha_3,\alpha_3=(u-\alpha_1)/v}. \tag{A6}$$

Note the appearance of the surface terms in form factors above. Being proportional to the Wandzura-Wilczek part of ϕ_{4K} and ψ_{4K}, they vanish for $m_K \to 0$.

The expressions for $f_{B_sK}^{+,0,T}$ form factors follows from above, by replacing u by $1-u$ and by interchanging α_1 and α_2, and m_d and m_s in the kaon DAs, i.e., by replacing DAs of $\bar{K}^0$ by those for K^0.

APPENDIX B: PARAMETERS USED IN THE CALCULATION

In this appendix we summarize the parameters used in the calculation of $f_{B_{(s)}K}$ form factors as well as in the calculation of $f_{B_{(s)}}$, Tables I, II, and III. For DAs, the parameters and their μ dependence are taken from [14,19]. The $\overline{MS}$ mass $\bar{m}_b$ entering the calculation is [33]

TABLE I. Input parameters for the kaon DA's [14,19].

Parameter	Value at $\mu = 1$ GeV
$\bar{m}_s$	128 ± 21 MeV
a_1^K	0.10 ± 0.04 [32]
a_2^K	0.25 ± 0.15
$a_{>2}^K$	0
f_{3K}	0.0045 ± 0.0015 GeV^2
ω_{3K}	-1.2 ± 0.7
λ_{3K}	1.6 ± 0.4
δ_K^2	0.20 ± 0.06 GeV^2
ω_{4K}	0.2 ± 0.1
κ_{4K}	-0.09 ± 0.02

TABLE II. Additional input parameters for the f_B and f_{B_s} sum rules.

Parameter	Value
$\alpha_s(m_Z)$	0.1176 ± 0.002
$\langle\bar{q}q\rangle$ (1 GeV)	$-(246^{+18}_{-19}$ MeV$)^3$
$\langle\bar{s}s\rangle/\langle\bar{q}q\rangle$	0.8 ± 0.3
$\langle\alpha_s/\pi GG\rangle$	$0.012^{+0.006}_{-0.012}$ GeV^4
m_0^2	0.8 ± 0.2 GeV^2

TABLE III. Three-particle twist-4 parameter relations for kaon DA's derived from the renormalon model [19,24].

$\phi_0^K = 0$	$\tilde{\phi}_0^K = -\frac{1}{3}\delta_K^2$	$\psi_0^K = -\frac{1}{3}\delta_K^2$	$\theta_0^K = 0$	$\Xi_0^K = \frac{1}{5}\delta_K^2 a_1^K$
$\phi_1^K = \frac{7}{12}\delta_K^2$	$\tilde{\phi}_1^K = -\frac{7}{4}\delta_K^2 a_1^K$	$\psi_1^K = \frac{7}{18}\delta_K^2$	$\theta_1^K = \frac{7}{10}\delta_K^2 a_1^K$	
$\phi_2^K = -\frac{7}{20}\delta_K^2 a_1^K$	$\tilde{\phi}_2^K = \frac{7}{12}\delta_K^2$	$\psi_2^K = \frac{7}{9}\delta_K^2$	$\theta_2^K = -\frac{7}{5}\delta_K^2 a_1^K$	

$$\bar{m}_b(\bar{m}_b) = 4.164 \pm 0.025 \text{ GeV}. \tag{B1}$$

The $\alpha_s(m_Z)$ value is the Particle Data Group (PDG) average [34]. There is a new value for the f_K decay constant [35], prepared for the PDG's 2008 edition,

$$f_K = (156 \pm 0.2 \pm 0.8 \pm 0.2) \text{ MeV}, \tag{B2}$$

which central value we adopt here, and the ratio of K^- and π^- decay constants is given by

$$\frac{f_K}{f_\pi} = 1.196 \pm 0.002 \pm 0.006 \pm 0.001. \tag{B3}$$

The $\bar{m}_s$ mass is the average [32] of the QCD sum rule determinations from [36,37] and covers the $\bar{m}_s$ mass range given the most recently in [38]. For the twist-2 kaon DA we use the first Gegenbauer moment a_1^K calculated at next-to-next-to-leading order accuracy from [32]. Since the existing fits and calculations for the value of the second Gegenbauer moment a_2^K show small SU(3) violation, with the large error, we accept here that $a_2^K = a_2^\pi$, with the value for a_2^K given in Table I [19]. We also use $m_K = 497.648 \pm 0.022$ MeV, $m_B = 5279.5 \pm 0.5$ MeV, and $m_{B_s} = 5366.1 \pm 0.6$ MeV [34].

[1] I. I. Balitsky, V. M. Braun, and A. V. Kolesnichenko, Nucl. Phys. **B312**, 509 (1989); V. M. Braun and I. E. Filyanov, Z. Phys. C **44**, 157 (1989); V. L. Chernyak and I. R. Zhitnitsky, Nucl. Phys. **B345**, 137 (1990).
[2] V. M. Belyaev, A. Khodjamirian, and R. Rückl, Z. Phys. C **60**, 349 (1993).
[3] V. M. Belyaev, V. M. Braun, A. Khodjamirian, and R. Rückl, Phys. Rev. D **51**, 6177 (1995).
[4] A. Khodjamirian, R. Rückl, S. Weinzierl, and O. I. Yakovlev, Phys. Lett. B **410**, 275 (1997).
[5] E. Bagan, P. Ball, and V. M. Braun, Phys. Lett. B **417**, 154 (1998).

[6] P. Ball, J. High Energy Phys. 09 (1998) 005.
[7] A. Khodjamirian, R. Rückl, and C. W. Winhart, Phys. Rev. D **58**, 054013 (1998).
[8] A. Khodjamirian, R. Rückl, S. Weinzierl, C. W. Winhart, and O. I. Yakovlev, Phys. Rev. D **62**, 114002 (2000).
[9] Z. H. Li, F. Y. Liang, X. Y. Wu, and T. Huang, Phys. Rev. D **64**, 057901 (2001).
[10] P. Ball and R. Zwicky, J. High Energy Phys. 10 (2001) 019.
[11] P. Ball and R. Zwicky, Phys. Rev. D **71**, 014015 (2005).
[12] A. Khodjamirian, T. Mannel, and N. Offen, Phys. Lett. B **620**, 52 (2005); Phys. Rev. D **75**, 054013 (2007).
[13] F. De Fazio, T. Feldmann, and T. Hurth, Nucl. Phys. **B733**, 1 (2006); J. High Energy Phys. 02 (2008) 031.
[14] G. Duplančić, A. Khodjamirian, T. Mannel, B. Melić, and N. Offen, J. High Energy Phys. 04 (2008) 014.
[15] M. Jamin and B. O. Lange, Phys. Rev. D **65**, 056005 (2002).
[16] C. W. Chiang, M. Gronau, and J. L. Rosner, Phys. Lett. B **664**, 169 (2008).
[17] A. Khodjamirian, T. Mannel, and M. Melcher, Phys. Rev. D **68**, 114007 (2003); **70**, 094002 (2004).
[18] X. G. Wu, T. Huang, and Z. Y. Fang, Phys. Rev. D **77**, 074001 (2008).
[19] P. Ball, V. M. Braun, and A. Lenz, J. High Energy Phys. 05 (2006) 004.
[20] V. M. Braun and I. E. Filyanov, Z. Phys. C **48**, 239 (1990).
[21] P. Ball, J. High Energy Phys. 01 (1999) 010.
[22] J. Bijnens and A. Khodjamirian, Eur. Phys. J. C **26**, 67 (2002).
[23] V. M. Braun and A. Lenz, Phys. Rev. D **70**, 074020 (2004).
[24] V. M. Braun, E. Gardi, and S. Gottwald, Nucl. Phys. **B685**, 171 (2004).
[25] Mathematica, Version 5.2 (Wolfram Research, Inc., Champaign, IL, 2005).
[26] M. Okamoto, Proc. Sci., LAT2005 (2006) 013.
[27] M. Artuso *et al.*, arXiv:0801.1833.
[28] M. A. Ivanov, J. G. Korner, S. G. Kovalenko, and C. D. Roberts, Phys. Rev. D **76**, 034018 (2007).
[29] D. Melikhov and B. Stech, Phys. Rev. D **62**, 014006 (2000).
[30] M. Gronau, Phys. Lett. B **492**, 297 (2000).
[31] R. Fleischer, Phys. Rep. **370**, 537 (2002).
[32] K. G. Chetyrkin, A. Khodjamirian, and A. A. Pivovarov, Phys. Lett. B **661**, 250 (2008).
[33] J. H. Kühn, M. Steinhauser, and C. Sturm, Nucl. Phys. **B778**, 192 (2007).
[34] W. M. Yao *et al.* (Particle Data Group), J. Phys. G **33**, 1 (2006) and http://pdg.lbl.gov/.
[35] J. L. Rosner and S. Stone, arXiv:0802.1043.
[36] K. G. Chetyrkin and A. Khodjamirian, Eur. Phys. J. C **46**, 721 (2006).
[37] M. Jamin, J. A. Oller, and A. Pich, Phys. Rev. D **74**, 074009 (2006).
[38] C. A. Dominguez, N. F. Nasrallah, R. Rontsch, and K. Schilcher, J. High Energy Phys. 05 (2008) 020.